Hydrol. Earth Syst. Sci., 25, 3301–3317, 2021
https://doi.org/10.5194/hess-25-3301-2021

Hydrology and Earth System Sciences
Open Access
EGU

Long-term climate-influenced land cover change in discontinuous permafrost peatland complexes

Olivia Carpino[1], Kristine Haynes[1], Ryan Connon[2], James Craig[3], Élise Devoie[3], and William Quinton[1]

[1]Cold Regions Research Centre, Wilfrid Laurier University, Waterloo, Ontario N2L 3C5, Canada
[2]Environment and Natural Resources, Government of the Northwest Territories,
Yellowknife, Northwest Territories X1A 2L9, Canada
[3]Department of Civil and Environmental Engineering, University of Waterloo, Waterloo, Ontario N2L 3G1, Canada

Correspondence: Olivia Carpino (ocarpino@wlu.ca)

Received: 6 August 2020 – Discussion started: 22 September 2020
Revised: 11 May 2021 – Accepted: 24 May 2021 – Published: 16 June 2021

Abstract. The discontinuous permafrost zone is undergoing rapid transformation as a result of unprecedented permafrost thaw brought on by circumpolar climate warming. Rapid warming over recent decades has significantly decreased the area underlain by permafrost in peatland complexes. It has catalysed extensive landscape transitions in the Taiga Plains of northwestern Canada, transforming forest-dominated landscapes to those that are wetland dominated. However, the advanced stages of this landscape transition, and the hydrological and thermal mechanisms and feedbacks governing these environments, are unclear. This study explores the current trajectory of land cover change across a 300 000 km^2 region of northwestern Canada's discontinuous permafrost zone by presenting a north–south space-for-time substitution that capitalizes on the region's 600 km latitudinal span. We combine extensive geomatics data across the Taiga Plains with ground-based hydrometeorological measurements collected in the Scotty Creek basin, Northwest Territories, Canada, which is located in the medial latitudes of the Taiga Plains and is undergoing rapid landscape change. These data are used to inform a new conceptual framework of landscape evolution that accounts for the observed patterns of permafrost thaw-induced land cover change and provides a basis for predicting future changes. Permafrost thaw-induced changes in hydrology promote partial drainage and drying of collapse scar wetlands, leading to areas of afforestation forming treed wetlands without underlying permafrost. Across the north–south latitudinal gradient spanning the Taiga Plains, relatively undisturbed forested plateau–wetland complexes dominate the region's higher latitudes, forest–wetland patchwork are most prevalent at the medial latitudes, and forested peatlands are increasingly present across lower latitudes. This trend reflects the progression of wetland transition occurring locally in the plateau–wetland complexes of the Scotty Creek basin and informs our understanding of the anticipated trajectory of change in the discontinuous permafrost zone.

Highlights.

1. Conceptual framework developed to understand the trajectory of permafrost thaw-induced land cover change
2. Permafrost thaw-induced land cover change varies latitudinally across the plateau–wetland complexes of the discontinuous permafrost zone
3. Partial wetland drainage triggers ecohydrological and thermal feedbacks that promote reforestation after full permafrost thaw.

1 Introduction

Northwestern Canada is one of the most rapidly warming regions on Earth (Vincent et al., 2015; Box et al., 2019), and it is transitioning to a warmer state at a rate that appears to have no analogue in the historical record (Porter et al., 2019). This transition includes region-wide thaw and disappearance of permafrost at unprecedented rates (Rowland et al., 2010). The Taiga Plains ecoregion of northwestern Canada extends from 55 to 68° N and, as such, encompasses the spectrum of permafrost cover, from continuous to sporadic. Permafrost thaw in the Taiga Plains ecoregion

is especially pronounced in its lower latitudes, where the permafrost is relatively thin and warm, often already at the thaw point temperature (Biskaborn et al., 2019), indicating a state of disequilibrium with the current climate (Helbig et al., 2016a). For example, Kwong and Gan (1994) repeated the permafrost surveys of Brown (1964) in northern Alberta and the southern Northwest Territories (NWT) and found that the southern limit of permafrost occurrence had migrated northward by about 120 km over a period of 26 years. Beilman and Robinson (2003) estimated that 30 %–65 % of the permafrost has disappeared from the southern Taiga Plains in the preceding 150 years, most of which disappeared in the latter 50 years. The accelerated rates of permafrost warming and thaw observed in recent decades throughout the circumpolar region (Biskaborn et al., 2019), including all of northwestern Canada (Kokelj et al., 2017; Holloway and Lewkowiz, 2019), have dramatically transformed land covers in the southern Taiga Plains (Chasmer and Hopkinson, 2017).

Much of the southern Taiga Plains is occupied by peatland-dominated lowlands, a landscape of raised, black spruce (*Picea mariana*) tree-covered peat plateaus overlying thin (<10 m), ice-rich permafrost interspersed with permafrost-free, treeless wetlands. These permafrost-free wetlands are predominantly classified as channel fens and collapse scar wetlands, the latter of which is developed from thermokarst erosion of the plateaus (Robinson and Moore, 2000). Peat plateaus and collapse scar wetlands are typically arranged into distinct plateau–wetland complexes, which are separated by channel fens. Each of these major land cover types in the lowlands of the southern Taiga Plains have contrasting hydrological functions (Hayashi et al., 2004), and therefore, changes to their relative proportions on the landscape can affect water flux and storage at the basin scale (Quinton et al., 2011). Permafrost thaw underlying plateaus is driven by horizontal conduction and advection from adjacent wetlands, and vertical heat flows from the ground surface (Walvoord and Kurylyk, 2016). As this permafrost thaws, the overlying plateau ground surface subsides and is engulfed by the surrounding wetlands (Beilman et al., 2001; Quinton et al., 2011; Helbig et al., 2016a). As such, permafrost thaw in this environment transforms forests to treeless, permafrost-free wetlands (Robinson and Moore, 2000). In the process, this also changes the hydrological function of the transformed land cover, in part due to a change in surface water–groundwater interactions (McKenzie and Voss, 2013). Such a transformation can profoundly affect local drainage processes and pathways (Connon et al., 2014, 2015), with implications to regional hydrology (St. Jacques and Sauchyn, 2009; Korosi et al., 2017; Connon et al., 2018), ecology (Beilman, 2001), biogeochemical processes (Gordon et al., 2016), and carbon cycling (Vonk et al., 2019; Helbig et al., 2016a).

Zoltai (1993) described a perpetual cycle of permafrost development and thaw in which permafrost evolves from perennial ice bulbs that form below *Sphagnum* hummocks in permafrost-free treeless wetlands (i.e. collapse scars). Such hummocks expand and coalesce, eventually forming tree-covered plateaus. However, over time plateaus experience a disturbance (e.g. fire and disease) that initiates the development of collapse scars, and as a result, the plateau or portions of it revert to a permafrost-free wetland. In a stable climate, the permafrost and permafrost-free fractions of a landscape are assumed to remain relatively consistent. Zoltai (1993) estimated that the time required to complete this cycle is approximately 600 years. Treat and Jones (2018) indicated timescales for forest recovery following permafrost thaw in the range of 450 to 1500 years. However, there is growing evidence throughout the southern Taiga Plains that the climate warming of recent decades has disrupted the cycle of permafrost thaw and redevelopment such that the rates of permafrost loss greatly exceed those of permafrost development (e.g. Halsey et al., 1995; Robinson and Moore, 2000; Quinton et al., 2011).

The accelerated rates of permafrost thaw and resulting land cover change described above call into question the utility of existing concepts (e.g. Zoltai, 1993) as a means to estimate the current trajectory of land cover change since such concepts were developed from analyses of geological sediments (e.g. peat cores) which generally lack the resolution needed to identify land cover change sequences over relatively short (i.e. decadal) periods. Moreover, it is uncertain whether the current rates of climate warming are represented in the sediment record. As a result, there remains considerable uncertainty on the trajectory of permafrost-thaw-induced land cover change in this region, including possible end-members and intermediate stages. Because of the close connection between land cover type and hydrological function in this region, the uncertainty related to possible land cover change trajectories also raises new uncertainties in regards to the region's water resources.

In addition to unprecedented climate warming in the north, accelerated permafrost thaw is also driven by positive feedbacks, including increased fragmentation of forested peat plateaus with increasing thaw (Chasmer et al., 2011), a process which increases the length of interface between permafrost and permafrost-free terrain and, therefore, also increases the overall flux of energy into the remaining permafrost bodies (Kurylyk et al., 2016). Connon et al. (2018) demonstrated that talik layers situated between the active layer and underlying permafrost are widespread in thawing peatland-dominated terrains, and their occurrence increases with increasing permafrost thaw. Devoie et al. (2019) demonstrated that once a talik forms, the rate of permafrost thaw can increase 10-fold.

Since the permafrost table beneath peat plateaus rises above the water surface of the adjacent wetlands, plateaus function as "permafrost dams" that prevent wetlands from draining. Permafrost thaw therefore removes this effect and enables previously impounded wetlands to partially drain until the hydraulic gradient driving their partial drainage

reaches an equilibrium state (Haynes et al., 2020). The slow release of water from the long-term storage of wetlands no longer impounded by permafrost changes the physical and ecological characteristics and hydrological function of these wetlands (Haynes et al., 2020). Such drainage transforms the uniformly wet *Sphagnum* lawns that characterize impounded wetlands, into hummocky surfaces that provide a wider range of near-surface moisture conditions, including those sufficiently dry to support the regrowth of trees (Haynes et al., 2020). There is also evidence that, when black spruce forest is lost due to permafrost thaw and plateau inundation, forest regeneration does not depend on the regeneration of permafrost (Haynes et al., 2020; Chasmer and Hopkinson, 2017). For example, treeless collapse scars have transformed into black spruce forest within 2–3 decades after the permafrost dams disappear (Haynes et al., 2018).

In addition to the transient drainage process described above that may occur following the removal of the impounding permafrost (Haynes et al., 2018), such removal also increases the hydrological connectivity of basins through the incorporation of wetlands that were previously impounded and, therefore, hydrologically isolated from the basin drainage network (Connon et al., 2015). This process of "wetland capture" expands the runoff contributing areas of basins, a process that increases their runoff potential. Connon et al. (2018) attributed the trends of increasing runoff ratio (i.e. fraction of basin runoff per unit input of precipitation) in basins throughout the Taiga Plains to this permafrost-thaw-induced process of runoff contributing area expansion.

The transition of one type of ground cover to another as a result of permafrost thaw or a subsequent process, such as partial wetland drainage and reestablishment of forest, also results in a change in surface energy balance (Kurylyk et al., 2016; Devoie et al., 2019). Insight into the nature of such changes can be obtained through comparing the energy regimes of the existing suite of land covers, including the end-members of land cover change. For example, the incoming solar radiation measured at a height of 2 m above the ground surface is highest in the treeless wetlands and lowest in areas of peat plateaus with dense forest (Haynes et al., 2019). The average shortwave radiation flux density of treeless wetlands is approximately twice of that measured below dense forest (Haynes et al., 2019). Plateau areas with moderate or sparse tree canopies have incoming solar radiation values intermediate between these two end-members (Chasmer et al., 2011). The ground surface albedo varies over the narrow range of 0.15 to 0.19 (Hayashi et al., 2007) among the ground surface types discussed here, with the exception being the late snowmelt period while plateau ground surfaces are still snow covered and the treeless wetlands are snow-free (Disher et al., 2021; Connon et al., 2021).

The nature of changes to a land cover's surface energy balance is governed by the properties of its subsurface, ground surface, and the overlying tree canopy, all of which change as one land cover type transitions to another (Helbig et al., 2016b). The reduction in the areal cover of forested plateaus and the concomitant increase in the coverage of treeless wetlands indicates that, in the first instance, permafrost thaw increases the incoming shortwave flux to the transformed land cover (Kurylyk et al., 2016; Devoie et al., 2019). Chasmer et al. (2011) found that this thaw-induced transition and associated increase of incoming shortwave radiation occurs over several years as tree mortality decreases the density of tree canopies. However, the forests that subsequently reestablish in partially drained wetlands may have an energy balance that shares some characteristics of the forested peat plateaus where insolation is relatively low, and the low albedo (and therefore high energy adsorption) of trunks, branches, and stems results in relatively high longwave and sensible heat compared to the treeless wetland surfaces (Helbig et al., 2016b).

Unprecedented climate warming and the feedbacks to thaw and land cover change are new factors not accounted for in current theories on permafrost degradation–aggregation cycles, based on the analysis of peat cores. As a result, the timescales for land cover transformations derived from such theories cannot account for the current rates and patterns of all thaw-induced land cover change. This study examines peat plateau–wetland complexes along a latitudinal gradient through the Taiga Plains to improve the understanding of permafrost thaw-driven land cover change in this region and to advance the ability to predict land cover changes over the coming decades. This overall objective will be accomplished by (1) delineating the current extent of peatlands and forest distribution along the latitudinal span of discontinuous permafrost, (2) characterizing the end-members and intervening stages of land cover transition, (3) providing an interpretation of the hydrological and ground surface energy balance regimes for each stage of land cover transition based on 20 years of field studies at the Scotty Creek Research Station, and (4) presenting a conceptual framework of peatland transition during and following permafrost thaw.

2 Study site

2.1 The Taiga Plains ecozone

Much of northwestern Canada's boreal region is located within the discontinuous permafrost zone, which ranges latitudinally from extensive-discontinuous permafrost (50 %–90 % areal permafrost coverage) in the north to sporadic-discontinuous permafrost (10 %–50 %) in the south. Within this region, the Taiga Plains ecozone contains a patchwork of mineral and organic terrain. This study examines the peat plateau collapse scar wetland complexes that dominate the lowlands of this ecoregion (Wright et al., 2009; Helbig et al., 2016a). While air temperature is the predominant control on permafrost, relatively dry peat at the ground surface can allow permafrost to exist where mean annual air temperatures

(MAATs) are at or even above 0 °C due to thermal insulation (Vitt et al., 1994; Camill and Clark, 1998). Permafrost is therefore largely restricted to below peat plateaus since only these features contain unsaturated layers sufficiently developed to insulate permafrost (Zoltai and Tarnocai, 1975; Hayashi et al., 2004; Quinton et al., 2009). The areal coverage of permafrost in the discontinuous zone has significantly decreased in recent decades due to increasing MAATs and has resulted in a shift towards more wetland-dominated landscapes (Thie, 1974; Robinson and Moore, 2000; Wright et al., 2009; Quinton et al., 2011; Olefeldt et al., 2016).

The discontinuous permafrost zone of the Taiga Plains ecozone covers 312 000 km^2 and, for the purposes of this study, is divided into the areas of extensive-discontinuous permafrost (151 000 km^2) and sporadic-discontinuous permafrost (161 000 km^2; Brown et al., 2002; Fig. 1). The Taiga Plains, bounded by the Taiga Cordillera to the west and Taiga Shield to the east, has a dry continental climate with short summers and long, cold winters with MAATs ranging from −5.5 to −1.5 °C (Vincent et al., 2012). MAATs have increased across the Taiga Plains over the past 50 years (1970–2019; Vincent et al., 2012) in a manner consistent with pan-Arctic warming (Overland et al., 2019). This is largely due to increases in average winter and spring temperatures of approximately 3 °C over this period (Vincent et al., 2012). However, there has been no consistent trend in mean annual precipitation over this period in the Taiga Plains (Mekis and Vincent, 2011).

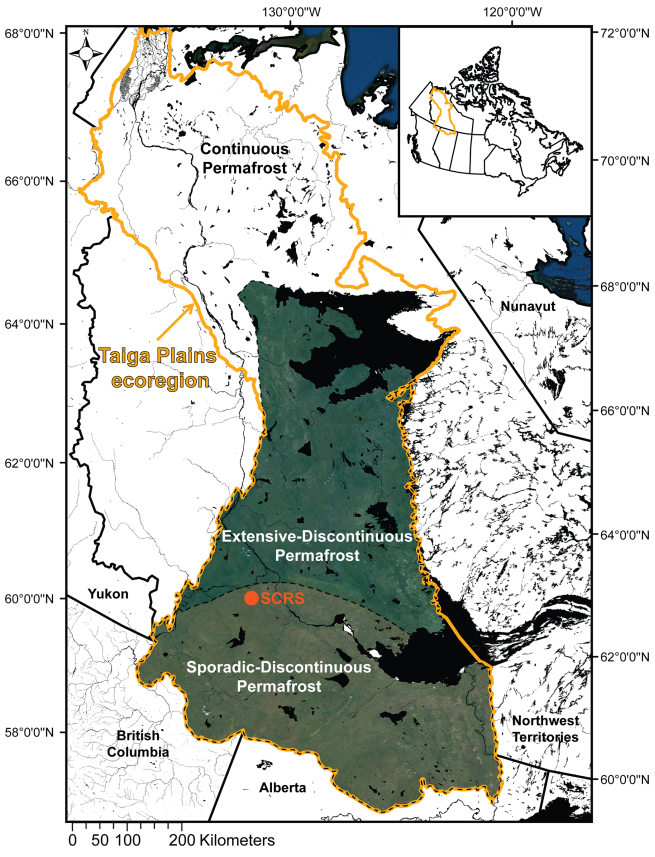

Figure 1. The Taiga Plains ecoregion with the discontinuous permafrost zones (coloured) defining the study region (Brown et al., 2002). The location of Scotty Creek Research Station (SCRS) is also indicated. This figure contains information licensed under the Open Government Licence – Canada.

2.2 Scotty Creek, Northwest Territories

Scotty Creek (61.3° N, 121.3° W) has been the focus of field studies and monitoring since the mid-1990s, and as such, the long-term and detailed data archive at Scotty Creek (Haynes et al., 2019) provides a unique opportunity to evaluate land cover changes over a period that coincides with rapid climate warming. Scotty Creek therefore also provides a reference to interpret land cover changes for terrains that are also present throughout the region. Scotty Creek is located approximately 50 km south of Fort Simpson, Northwest Territories (Fig. 1), where the MAAT (1970–2015) is −2.6 °C, and the mean annual precipitation (1970–2015) is 400 mm, of which 150 mm falls as snow (Environment and Climate Change Canada, 2020). Data collected by Environment and Climate Change Canada at the Fort Simpson A climate station show that MAAT has increased by approximately 0.05 °C per year since 1950, with warming most pronounced during the winter. Scotty Creek drains a 152 km^2 area dominated by peatlands, with peat accumulations ranging between 2 and 8 m overlying a clay- and silt-rich glacial till (McClymont et al., 2013). The Scotty Creek drainage basin occupies one of many peatland-dominated lowlands of the Taiga Plains, and as such, its landscape is dominated by complexes containing tree-covered peat plateaus overlying permafrost alongside treeless and permafrost free collapse scar wetlands. Such plateau–wetland complexes are separated by channel fens that collectively function as the basin drainage network (Hayashi et al., 2004; Quinton et al., 2009). This type of land cover not only dominates the lowlands of the Taiga Plains but is also found extensively throughout northwestern Canada and across the circumpolar subarctic (Olefeldt et al., 2016).

3 Methods

3.1 Geomatics methods

To place Scotty Creek into a regional context, geomatics methods were applied to both zones of discontinuous permafrost within the Taiga Plains to quantify the areas occupied by each of the major land covers of all areas identified as peatland-dominated lowland. Multispectral Landsat 8 imagery (30 m resolution; Fig. 2a) was acquired across an area of over 300 000 km^2 totalling 70 Landsat scenes. Of these, 59 scenes were used to construct the base of the mosaic, and 11

were used as secondary data to patch and minimize cloud cover. The 59 primary scenes were acquired in 2017 and 2018, while the 11 secondary scenes were acquired between 2013 and 2016 as data of suitable quality were unavailable during the preferred time period. Acquiring imagery during the snow-free season was prioritized, and as such, all 70 Landsat tiles were acquired in June, July, or August, rendering the coniferous forest cover seasonally comparable and allowing for a more streamlined mosaicking process. A colour infrared mosaic (Landsat 8 bands 5, 4, and 3, displayed as R, G, and B; Fig. 2b) was created across the study region in ArcGIS (Esri, Redlands, California, USA) using a Lambert conformal conic projection. The mosaic data set was colour balanced, and the boundary was amended to the Taiga Plains ecozone, including the delineations dividing the sporadic and extensive discontinuous zones (Brown et al., 2002).

To determine the current distribution of the peatland-dominated lowlands that contain the same type of terrain as observed at Scotty Creek (i.e. plateau–wetland complexes separated by channel fens), two complementary products were used in the ArcGIS suite of programmes. First, a Natural Resources Canada saturated soils data set (Fig. 2c; Natural Resources Canada, 2017) was selected to isolate areas that were wetland dominated and likely representative of the plateau–wetland complexes targeted in this study. Next, the Northern Circumpolar Soil Carbon Database (NCSCD;Fig. 2d; Bolin Centre for Climate Research, 2013) was selected to determine whether the highlighted wetland-dominated areas are also likely to represent peatland-dominated areas.

The saturated soils data set is part of a larger digital cartographical project of Natural Resources Canada, CanVec. The CanVec data set is a vector format data set, which can be downloaded by province/territory or Canada-wide, and includes over 60 features organized into eight themes, including land features. Land features in this data set, such as the distribution of saturated soils, were originally digitized at a scale of 1 : 50000 (Natural Resources Canada, 2017). The NCSCD is also a polygon database developed by the Bolin Centre for Climate Research through synthesizing data from numerous regional and national soil maps alongside field data collected across Canada, USA, Russia, and the European Union. The NCSCD includes data on the fractional coverage of different soil types and stored soil organic carbon (Hugelius et al., 2013a, b). In the present study, the layer containing information on the fractional coverage of soil types was used. While the original format of the NCSCD is a vector of delineated zones, gridded data are also available at resolutions varying from 0.012 to 1° (Hugelius et al., 2013b). The NCSCD is comprised of a circum-Arctic data set and country-wide and regional data sets, including one of Canada (Hugelius et al., 2013b).

The NCSCD is a widely used data set (Olefeldt et al., 2014; Gibson et al., 2018; Stofferahn et al., 2019; etc.), but the zones do not map specific locations of peatland-dominated terrain (Fig. 2d). The locations of peatlands are helpful for work in regions such as the Taiga Plains, where the landscape is a patchwork of both organic and mineral terrain. The saturated soils data set and the NCSCD were then both masked to the Taiga Plains boundaries in ArcGIS, where over 26 000 saturated soil polygons and 572 NCSCD zones were contained within the study region. The saturated soils data set was mapped to display probable peatland terrain across the study region (Fig. 2c). The areas of each saturated soil polygon were calculated alongside the areas for each NCSCD zone using the boundaries in the data set. As the fractional coverage product from the NCSCD was used in this study, the fractional area of probable peatland terrain within the same NCSCD zone was calculated. The fractional areas of organic soils reported in the NCSCD were then compared to the fractional areas of probable peatland terrain from the saturated soils data set within the same NCSCD zone boundary (Fig. 2e).

The Landsat mosaic data set (Fig. 2b) was then combined with the resultant product displaying peatland terrain (Fig. 2e). An unsupervised land cover classification was subsequently completed on the Landsat mosaic across the areas identified by the saturated soils and NCSCD data sets to identify and classify the land covers within these peat plateau–wetland complexes (Fig. 2f). The first iteration of the unsupervised classification (Iso Cluster classification approach) targeted 50–75 classes (72 created). The original 72 classes were then aggregated into 12 final classes within the peatland terrain outlined across the Taiga Plains study region. The final 12 aggregated classes include coniferous (dense and sparse), mixed (dense and sparse) and broadleaf forests stands (dense and sparse), collapse scar, fen, open water, bare ground, cloud, and cloud shadow.

Forested peatlands are particularly indicative of landscape change in this region (Quinton et al., 2011; Baltzer et al., 2014; Chasmer and Hopkinson, 2017), and as such, identifying the forested areas within the already identified peatland-dominated terrain was the focus of the Landsat classification. Specifically, the proportion of coniferous forested area within the total peatland area was quantified across the region's latitudinal span (Fig. 2g). Fractional coniferous forested area was selected rather than total forested area to account for the observed spatial differences in peatland distribution across the Taiga Plains. For each degree of latitude, a bin was created for the fractional forested area, and the median was calculated alongside upper (i.e. 75th percentile) and lower (i.e. 25th percentile) quartiles. These data were plotted as a function of latitude across the Taiga Plains ecozone. This generated a data set of forest cover across the peatland-dominated regions of interest that was subsequently complemented by field data collected in the Scotty Creek basin to guide the proposed conceptual framework.

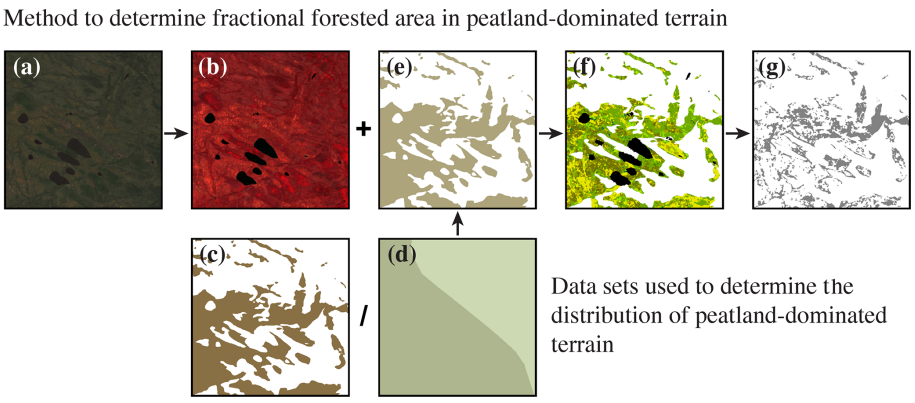

Figure 2. A summary of the regional geomatics methods used over a 2 km × 2 km sample area. There are two main workflows highlighted, i.e. the data sets used to map probable peatland-dominated terrain and the methods used to determine fractional forested area within those peatland-dominated areas. **(a)** Multispectral Landsat 8 imagery. **(b)** False colour infrared Landsat 8 imagery. **(c)** Natural Resources Canada saturated soils data set. **(d)** Northern Circumpolar Soil Carbon Database (NCSCD) fractional area of organic soils. **(e)** Probable peatland-dominated terrain. **(f)** Unsupervised classification identifying land covers within peatland-dominated terrain. **(g)** Coniferous forest cover within peatland-dominated terrain.

3.2 Scotty Creek imagery

To help capture examples of the stages of the transitioning landscape, imagery was collected using a remotely piloted aircraft system (RPAS) across the Scotty Creek basin to represent how each of these illustrated trajectory stages manifests on the landscape in a peat plateau and collapse scar wetland-dominated environment. The RPAS imagery (0.5 m resolution) was collected in the summer of 2018 using an eBee Plus drone equipped with a senseFly S.O.D.A. 3D mapping camera, and all image processing was completed in Pix4Dmapper.

Imagery for Scotty Creek, including aerial photographs from 1947, 1970, and 1977, IKONOS satellite imagery from 2000, and WorldView satellite imagery from 2010 and 2018 were used to quantify the area occupied by peat plateaus, collapse scar wetlands, and channel fens in each of these years. The aerial photographs (0.5-1.2 m resolution) and IKONOS imagery (4 m resolution) were previously classified, and the results were presented in Quinton et al. (2011). Carpino et al. (2018) completed the land cover classifications for the 2010 WorldView imagery, and Disher (2020) classified the 2018 WorldView imagery. Collectively, these images document the land cover change at the Scotty Creek basin over the period from 1947 to 2018.

3.3 Hydrological data

A comprehensive archive of hydrometeorological measurements was used in this study to examine the temporal variation in hydrological characteristics as land cover transitions from one stage to another. The form and hydrological function of the major land cover types of permafrost plateau, collapse scar, and channel fen are well understood from numerous studies at Scotty Creek since the 1990s (Quinton et al., 2019). Field studies and monitoring at Scotty Creek over this period have also provided firsthand accounts of how permafrost thaw changes land covers (Quinton et al., 2019). In the present study, we examined how runoff, evapotranspiration, and water storage are affected as land cover changes. In addition, we examined the precipitation data collected from 2008 to 2019 (Geonor, Model T200B) in relation to the three hydrological components listed above to gain insights into how changes in land cover affect the water balance for each stage in the land cover transition. These stages will be presented in detail in Sect. 4.2. The Geonor precipitation data include both rain and snow measurements logged at 30 min intervals (Table 1). Monitoring of discharge from Scotty Creek by the Water Survey of Canada began in 1996. For this study, annual basin runoff (millimetres per year) between 1996 and 2015 was calculated and used in the basin runoff component of the conceptual framework (Table 1; Connon et al., 2014; Haynes et al., 2018). Given that this period of discharge monitoring coincided with a period of considerable climate warming and documented land cover change at Scotty Creek, the trend in calculated runoff over the period of record reflects a shift from a permafrost-plateau-dominated landscape to one increasingly influenced by hydrologically connected wetlands. Therefore, the temporal trend of runoff from the Scotty Creek basin is driven by permafrost-thaw-induced land cover change (Connon et al., 2014; Haynes et al., 2018).

Recent work by Warren et al. (2018) examined evapotranspiration (ET) for forests, wetlands, and the integrated landscape within the Scotty Creek watershed between 2013 and 2016. Daily ET values (millimetres per day) reported by Warren et al. (2018) were converted to annual ET (millimetres per year) for the purpose of the conceptual framework water balance in the present work (Table 1). The different land

Table 1. Annual precipitation (2008–2019), basin runoff (1996–2015; Connon et al., 2014; Haynes et al., 2018), evapotranspiration (2013–2016; Warren et al., 2018), and residual storage values are presented (millimetres per year) for two distinct transitional landscape stages at Scotty Creek, namely a landscape dominated by forest and a patchwork landscape of near-equal forest and treeless wetland land covers.

	Forest > Wetland	Forest ≈ Wetland
Precipitation	493	493
Runoff	149	215
Evapotranspiration	206	255
Residual storage	138	23

covers monitored by Warren et al. (2018) are representative of the land cover end-members identified in our conceptual framework. Therefore, the annual ET values based on the data collected by Warren et al. (2018) for the black spruce forests, open collapse scar wetlands, and the integrated landscape were associated with the appropriate stage along our proposed trajectory of change. Stages of the trajectory for which representative measurements were not collected are interpolated between the land cover end-members for which ET was measured.

Given the insignificant changes in annual precipitation over the period of measurement (Connon et al., 2014; Haynes et al., 2018), annual storage was calculated as the residual of annual precipitation inputs, and annual evapotranspiration and runoff outputs for the conceptual framework water balance (Table 1).

3.4 Radiation fluxes

A total of four meteorological stations at Scotty Creek were selected for use in this study (Fig. 3). This included a station installed in a collapse scar wetland in 2004 (hereafter wetland station) followed by a second station on a densely forested peat plateau in 2007 (hereafter dense forest station). The radiation flux data from these two stations are representative of the collapse scar wetland and permafrost plateau land cover types, respectively. Furthermore, two additional stations located on forested plateaus were also used to represent tree canopy densities different from that of the dense forest station. These stations were installed on a sparsely forested peat plateau in 2015 (hereafter sparse forest station) and a forested plateau with a canopy of intermediate density between that of the dense and sparse stations in 2014 (hereafter intermediate forest station). All radiation measurements were made below the tree canopy at a height of 2 m above the ground surface. Radiation fluxes in the form of four component radiation data were collected at the dense forest, sparse forest, and wetland meteorological stations, while only shortwave radiation was collected at the intermediate forest station. The reader is directed to Haynes et al. (2019) for full descriptions of the radiation instrumentation within the Scotty Creek basin. Radiation was measured every minute and averaged and recorded every 30 min from which daily (24 h) averages were computed. The daily averages were then used to compute annual average radiation for each station. While these computations defined some of the variability in radiation fluxes among land cover types, they do not account for flux variations over short temporal and spatial scales (Webster et al., 2016). To address these, the daily average four component radiation data from each station were compared on a monthly time step. The monthly averages were calculated and compared across the land covers represented by each of the four meteorological stations using a one-way analysis of variance (ANOVA) with Tukey post hoc test ($\alpha = 0.05$), thereby testing the effect of land cover on monthly shortwave and longwave incoming and outgoing radiation.

4 Results and discussion

4.1 Peatland and forest occurrence

The type of peatland-dominated terrain composed of peat plateau–wetland complexes separated by channel fens as described for Scotty Creek, occupy approximately 35 % of the discontinuous permafrost zones of the Taiga Plains (Fig. 4a). Large peatland clusters are located in lowland areas with high histel or histosol soil percentages. In the extensive-discontinuous permafrost zone, peatlands are clustered to the west near to the Mackenzie River and are largely absent from the eastern portion of the study area in the region bounded by Great Bear Lake to the north and the Taiga Shield to the east. In the sporadic-discontinuous zone, however, the peatland clusters are more longitudinally dispersed.

Comparing the fractional areas of probable peatland terrain from the saturated soils data set to the NCSCD showed that the saturated soils data set was more likely to overstate the distribution of probable peatland terrain compared to the NCSCD maps. Approximately 20 % of the fractional areas were exact matches between the two data sets, 20 % were lower in the saturated soils data set, and 60 % were higher in the saturated soils data set. However, despite these disagreements, 79 % of the fractional areas determined using the saturated soils data set were within 15 % of the fractional areas in the NCSCD. This suggests that using the Natural Resources Canada saturated soils data set may be an appropriate method of mapping probable peatland terrain in the Taiga Plains on a finer scale (Fig. 4a) compared to the broad zones presented by the NCSCD (Fig. 4b). Only 11 of the 572 NCSCD zones (~ 2 %) had disagreements over 25 % when comparing the fractional areas between both data sets. The majority of these zones of disagreement were located along the Slave River, in the far southeast of the Taiga Plains study region.

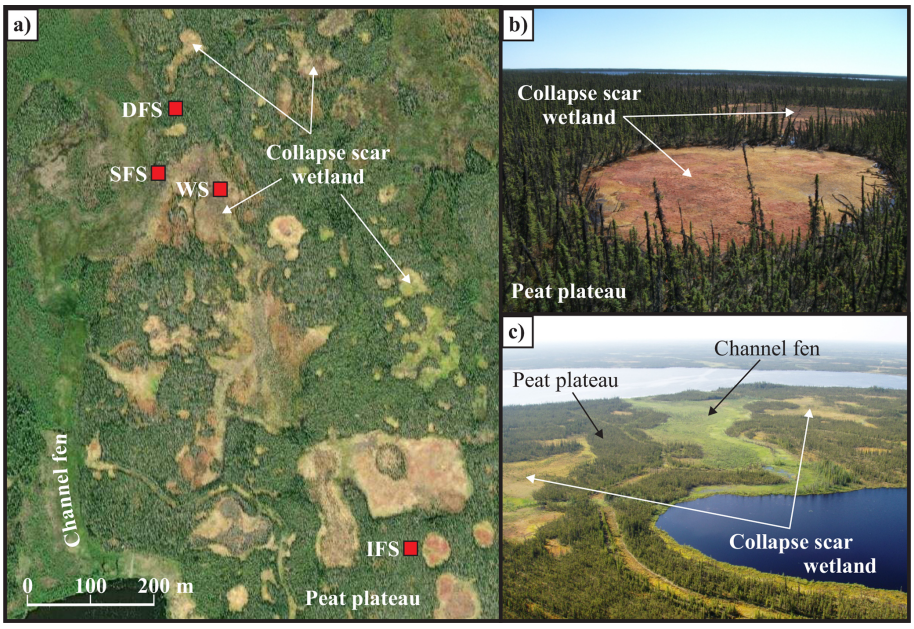

Figure 3. WorldView 2 satellite image **(a)** and oblique aerial photographs **(b, c)** over Scotty Creek, Northwest Territories. The satellite image also shows the locations of the Dense Forest Station (DFS), Sparse Forest Station (SFS), Wetland Station (WS), and Intermediate Forest Station (IFS) micrometeorological stations. The oblique aerial photographs show the land cover types that dominate lowlands with discontinuous permafrost in the Taiga Plains, including peat plateau (permafrost), collapse scar wetland, and channel fen.

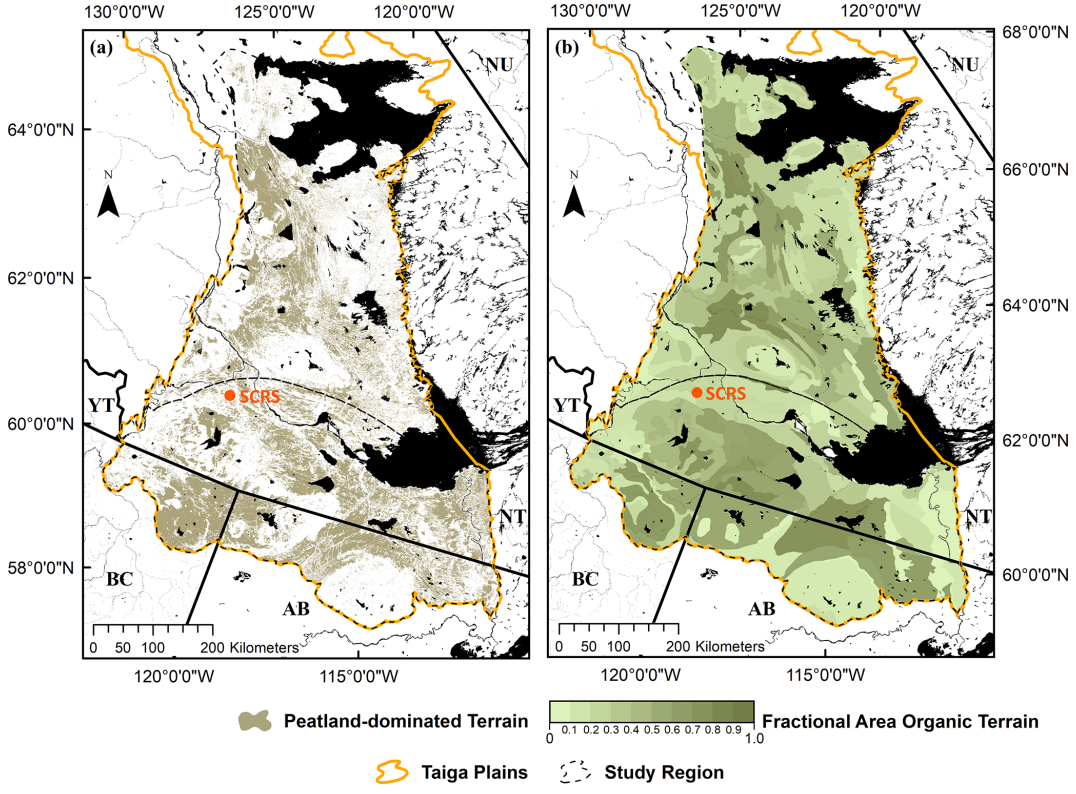

Figure 4. Predicted distribution of peatland-dominated terrain in the discontinuous permafrost zone of the Taiga Plains (**a**). Peatland-dominated terrain was mapped using a saturated soils data set (Natural Resources Canada, 2017) **(a)** and compared to the NCSCD (Bolin Centre for Climate Research, 2013) **(b)**. This figure contains information licensed under the Open Government Licence – Canada.

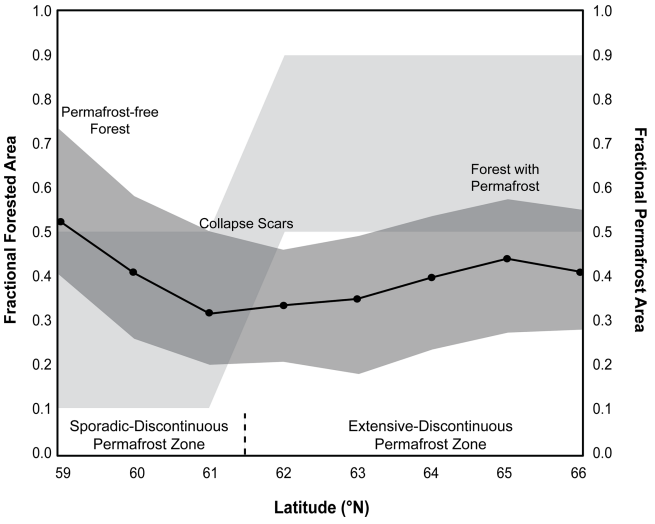

Figure 5. Median forested peatland area expressed as a fraction of the total peatland area and plotted as a function of latitude. The dark grey area represents the range in the proportion of the landscape occupied by forested peatland (i.e. fractional forested area) between the 25th percentile and 75th percentile. The lighter grey area indicates the range in the proportion of landscape underlain by permafrost (i.e. fractional permafrost area) as indicated by Brown et al. (2002).

A latitudinal trend in land cover percentage was found for the mapped peatland-dominated terrain (Fig. 5). Along the boundary between the extensive-discontinuous and sporadic-discontinuous permafrost zones near the centre of the study region, collapse scar wetland features are most prevalent. Median fractional forest cover in peatlands (i.e. peat plateaus or treed wetlands) reaches its minimum value of 33 % within the 61° N bin, near the latitude of Scotty Creek. The proportion of forested peatlands remains relatively low throughout the transitional zone between sporadic and extensive discontinuous permafrost (approximately 61 to 62° N), where the median forest cover does not exceed 34 %. The widespread occurrence of collapse scars suggest that permafrost thaw and the resulting processes of ground surface subsidence and inundation are particularly active in this zone compared to the extensive-discontinuous permafrost zone to the north and the sporadic-discontinuous permafrost zone to the south, where the fractional forested areas are higher.

The median proportion of forested peatlands in the extensive-discontinuous zone (63 to 66° N) ranges from approximately 35 % to 45 %, indicating that permafrost thaw is less prevalent over the landscape than in the transition zone immediately to the south. However, the median fractional forested area is at its greatest (52 %) south of the transition in the sporadic-discontinuous zone (59 to 60° N), where about half of the peatland area is forest covered. Expansion of forest cover in this zone, especially in the areas of northeastern British Columbia and northwestern Alberta, has been reported by others (e.g. Zoltai, 1993; Carpino et al., 2018). A pattern of forest expansion over permafrost-free terrain is consistent with the observation of a northward-moving southern limit of permafrost reported by Kwong and Gan (1994) and with the process of tree reestablishment following permafrost-thaw-induced partial drainage of wetlands described by Haynes et al. (2020).

4.2 Conceptual framework of land cover change

From the remote sensing and field-based hydrological studies at Scotty Creek since the mid-1990s, key insights into incremental land cover changes initiated by permafrost thaw have emerged. Using this knowledge as a foundation, the present study examines both the hydrological and radiation regimes of each incremental stage and the land cover changes over the larger region in which permafrost thaw is known to be widely occurring and within which the southern edge of permafrost is migrating northward (Kwong and Gan, 1994). From this approach, a new conceptual framework is presented (Fig. 6), which describes permafrost-thaw-induced land cover change in the peatland-dominated regions of the discontinuous permafrost zone. The land cover change occurring simultaneously (to varying degrees) at Scotty Creek and latitudinally across the wider Taiga Plains region can be categorized into seven distinct land cover stages, the first and last of which are forest cover, with the difference being that the former overlies permafrost and the latter does not. The stages are as follows: (I) forested permafrost plateaus, (II) forested permafrost plateaus with small, isolated collapse scars, (III) forested permafrost plateaus with larger, interconnected wetlands, (IV) wetland complexes with small plateau islands, (V) wetland complexes with hummock development and tree establishment, (VI) hummock growth with forest establishment, and (VII) forested peatlands (Fig. 6). In the following sections, the biophysical, hydrological, and radiation regimes of each of these stages are presented and discussed, drawing on several investigations in the region.

4.2.1 Biophysical characteristics

The present study found that the early land cover stages presented in Fig. 6 are more prevalent at the higher latitudes of the study region and the later stages at the lower latitudes. Considering that permafrost thaw is more advanced in the lower latitudes and that the southern limit of permafrost is advancing northward (Kwong and Gan, 1994), it is reasonable to expect that the more advanced stages presently characterizing the lower latitudes will, in the future, characterize the higher latitudes, assuming a continuation of climate-warming-induced permafrost thaw. Approaching a change in latitude through the study region as analogous to a change in land cover stage, or, more specifically, to a change in time, is supported by studies that examined land cover change over the last half-century at Scotty Creek (Chasmer and Hopkin-

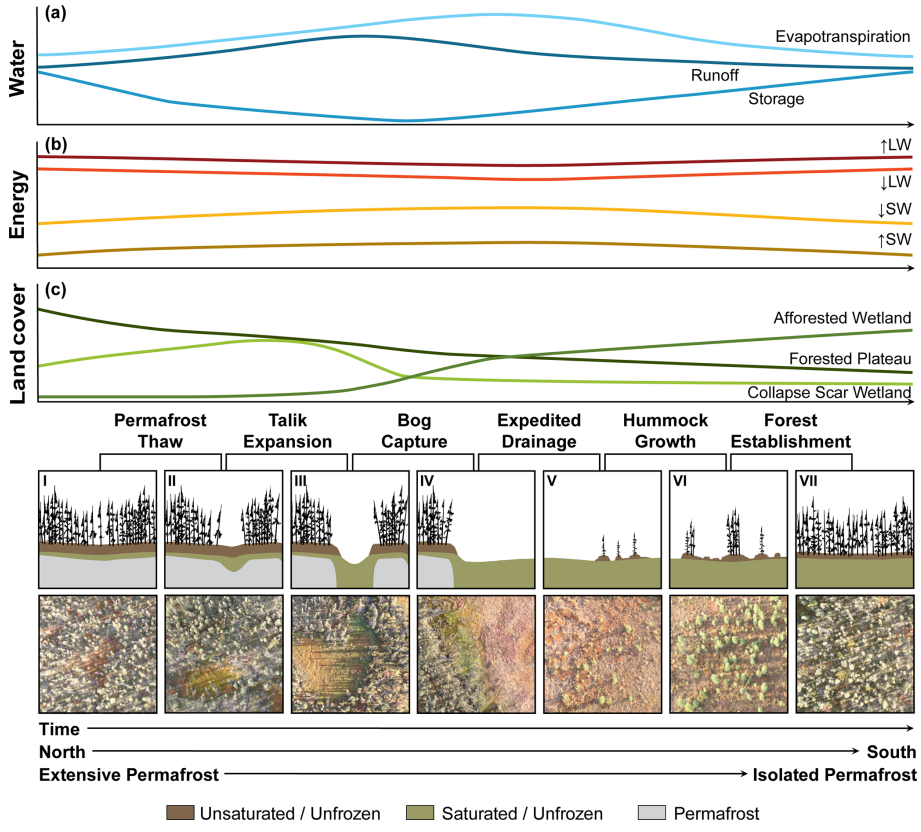

Figure 6. The graphic below the panels shows the proposed conceptual framework of landscape trajectory, including a space-for-time substitution for changes to both permafrost and land cover. Conceptual diagrams are presented to illustrate landscape change, with the support of RPAS imagery collected in the Scotty Creek basin. The conceptual framework is presented alongside the processes that initiate the trajectory's progression. **(a)** Relative changes to local water balances of measured Scotty Creek basin runoff, evapotranspiration, and residual storage with unchanging precipitation are summarized and presented over the trajectory of landscape change based on the proportion of forested vs. wetland area. **(b)** Relative changes to local energy balances are presented using data collected from subcanopy meteorological stations installed at Scotty Creek. **(c)** Changes to relative land cover proportions are presented using historical aerial photographs and recent acquisitions of satellite imagery over the Scotty Creek basin.

son, 2017; Quinton et al., 2019) and along a north to south transect extending from Scotty Creek to northeastern British Columbia (Carpino et al., 2018).

The Scotty Creek basin, located near the northern limit of sporadic discontinuous permafrost (Fig. 1), is characterized mainly by stages III and IV. However, examples of all seven stages can be found in local areas at Scotty Creek. For this reason, the long-term monitoring and research programmes at Scotty Creek involving each of these land cover types contributes detailed information on their form and functioning and on their transition from one to another. For example, permafrost thaw changes a landscape dominated by forested plateaus (Fig. 6I) to one with small, suprapermafrost taliks (Connon et al., 2018) and isolated collapse scars (Fig. 6II; Quinton et al., 2011). Continued thaw expands isolated collapse scars (Fig. 6III; Devoie et al., 2019), enabling them to coalesce to form interconnected wetlands (Connon et al., 2015), a process that then leads to a landscape of expansive wetlands dotted with isolated plateau "islands" (Fig. 6IV; Baltzer et al., 2014; Chasmer and Hopkinson, 2017). Since the process of wetland expansion removes peat plateaus, a land cover type that impounds wetlands and obstructs drainage (Connon et al., 2014), this process enables the landscape drain more efficiently (Haynes et al., 2018). As wetlands drain, hummock microtopography develops in their relatively drier interiors (Fig. 6V; Haynes et al., 2020), which allows black spruce to colonize the wetlands on the relatively dry hummock surfaces (Fig. 6VI; Iversen et al., 2018; Dymond et al., 2019). Continued drainage and drying of wetlands enables the expansion of their hummocky terrain and, therefore, of their tree cover (Eppinga et al., 2007; Iversen et al., 2018) until the landscape returns to a more continuous forest cover (Fig. 6VII; Carpino et al., 2018). However, the forest cover in this final stage is permafrost-free, and for that reason, the conceptual framework presented in Fig. 6 stands in contrast to those presented by Zoltai (1993) and Camill (1999) in which the reemergence of a forest cover relies on the reemergence of the underlying per-

mafrost. According to Zoltai (1993), forest reemerges because permafrost displaces the overlying ground surface upward, resulting in the development of an unsaturated layer suitable for tree establishment. In contrast, the tree establishment described in Fig. 6 results not from the reemergence of permafrost, but from its continued thaw over the landscape, a process that dewaters wetlands (Connon et al., 2014; Haynes et al., 2018) to the extent suitable for tree establishment (Haynes et al., 2020).

The land cover transition depicted in Fig. 6, involving wetland drainage and forest reestablishment, occurs in less than half a century, as indicated by an analysis of historical imagery for Scotty Creek. In contrast, the process of forest regrowth enabled by the reestablishment of permafrost occurs over a much longer time frame of several centuries (Zoltai, 1993; Treat and Jones, 2018). At Scotty Creek, the early stages of Fig. 6 (i.e. stages I and II) represent the changes observed between 1947 and 2000, over which time the tree-covered area decreased from approximately 70 % to approximately 50 % (Quinton et al., 2011). The fraction of forested land above the permafrost-free terrain cover is unknown for this period but is assumed to be negligible based on land cover descriptions for this region (e.g. NWWG, 1988; Zoltai 1993; Robinson and Moore, 2000). This period, therefore, generated a concomitant rise in the cover of wetlands over the landscape (i.e. 30 % to 50 %) since permafrost thaw transitions the tree covered plateaus to collapse scars and channel fens, as confirmed by analysis of archived imagery (Chasmer et al., 2010). By 2018, tree-covered peat plateaus decreased to 40 %, and treeless wetlands occupied 45 % of the land cover (13 % collapse scars and 32 % channel fens; Disher, 2020). These studies indicate that permafrost thaw and the resulting processes have both removed forest as a result of thaw-induced subsidence and the inundation of plateau surfaces and, more recently, enabled forest reestablishment in the form of treed wetlands (Haynes et al., 2020; Disher et al., 2021). However, the dominant land cover transition at Scotty Creek is still from forest (peat plateau) to wetland as a result of permafrost thaw, resulting in a net forest loss, a process that will continue until the later stages of Fig. 6 are reached (i.e. stages VI and VII), at which point there will be a net forest gain.

The sequence of land cover stages following permafrost thaw observed at Scotty Creek and depicted in Fig. 6 is supported by vegetation successional changes described in the literature for wetlands as they age. For example, aquatic *Sphagnum* species, notably *S. riparium*, are the first to occupy the inundated margins between thawing permafrost plateaus and developing collapse scars (Garon-Labrecque et al., 2015; Pelletier et al., 2017). Such recent areas of collapse are easily identified on high-resolution RPAS imagery by the distinct bright green colour of *S. riparium* (Fig. 6II, III, and IV; Gibson et al., 2018; Haynes et al., 2020). These wetland–plateau edges may also be identified by bare peat or moats of water (Zoltai, 1993). As collapse scars expand, lawn species, such as *S. angustifolium,* and hummock species, such as *S. fuscum*, emerge, particularly in the drier interior of wetlands (Zoltai, 1993; Camill, 1999; Pelletier et al., 2017). Hummock species, mainly *S. fuscum*, first emerge near the centre of collapse scars and expand outward over time (Camill, 1999; Loisel and Yu, 2013). Much like *S. riparium*, *S. fuscum* is also easily identified in high-resolution imagery, where *S. fuscum* is distinguished by its russet colour (Fig. 6V; Haynes et al., 2020). As the density of the *S. fuscum* hummocks increases, imagery and ground-based observations indicate the presence of young black spruce trees (Lieffers and Rothwell, 1987; Haynes et al., 2020), first on isolated hummocks (Fig. 6VI) but eventually as widespread afforestation (Fig. 6VII; Camill, 2000; Ketteridge et al., 2013).

4.2.2 Radiation flux characteristics

The Scotty Creek basin is a microcosm of its larger regional setting since it contains each of the land cover stages of the conceptual framework in Fig. 6. As such, the micrometeorological measurements made at Scotty Creek for different land cover types provide insight into how energy regimes change as one land cover stage transitions to the next. Both incoming and outgoing shortwave radiation peak at the middle stages (IV and V), where treeless collapse scars predominate. Annual incoming and outgoing shortwave radiation is lowest at the dense forest station, which represents the initial stage (I). Likewise, incoming and outgoing annual longwave radiation are greatest in the early (I and II) and late stages (VI and VII) and lowest in the wetland-dominated middle stages (IV and V).

Statistically significant differences were found between stations for incoming (Fig. 7a) and outgoing (Fig. 7b) shortwave and incoming longwave radiation (Fig. 7c), while there was no statistical differences between stations for outgoing longwave (Fig. 7d). However, Tukey post hoc tests revealed variability between the two shortwave components in terms of which groups showed these significant differences. As the four meteorological stations fall along a gradient of forest density from treeless wetland to a densely forested plateau, no significant differences in incoming shortwave radiation were ever found between stations only one rank apart on that gradient. As such, measurements indicate average monthly incoming shortwave radiation is significantly greater at the wetland compared to both the intermediate forest ($p<0.05$) and the dense forest ($p<0.05$), while no significant difference exists between wetland and the sparse forest. However, the dense forest receives significantly less incoming shortwave radiation than both the wetland ($p<0.05$) and the sparse forest ($p<0.05$), but this station is not significantly different from the intermediate forest.

No significant differences in outgoing shortwave radiation exist between any of the forested plateau stations, but all are significantly different from the wetland. Specifically, outgoing shortwave radiation recorded at the wetland station is sig-

nificantly greater than the sparse forest ($p<0.05$), intermediate forest ($p<0.05$), and dense forest stations ($p<0.05$). The differences between the wetland station and the forested plateau stations are also increasingly significant with increasing tree density. There was a statistically significant difference between the three stations (intermediate forest omitted due to lack of measurements) for incoming longwave radiation, while no statistically significant differences were observed in the outgoing longwave radiation component. The only significant difference in incoming longwave was observed between the wetland and dense forest ($p<0.05$). No significant differences exist between the sparse forest and the wetland or dense forest.

The comparison among the plateau stations of contrasting tree canopy densities provides insight into the permafrost-thaw-induced progression of radiation regimes as plateaus transition to wetlands, a process involving the gradual thinning and eventual loss of the tree canopy. Wright et al. (2009) demonstrated that small-scale changes to the tree canopy density can increase insolation to the ground in localized areas, leading to thaw depressions in the active layer and water flows toward such depressions from their surroundings. Such areas of preferential thaw therefore develop elevated soil moisture contents, and since soil thermal conductivity increases with its moisture content, the preferential thaw process is reinforced. This is suggested as the mechanism driving the transition from stage I to II in the trajectory (Quinton et al., 2019). This feedback is present in the initial stages of the trajectory and is often associated with talik formation and expansion into collapse scars due to localized permafrost loss (Chasmer and Hopkinson, 2017; Connon et al., 2018). Such thaw can extend to the base of the active layer, in which case further thaw results in permafrost loss, ground surface subsidence, waterlogging of the ground surface, local tree mortality, and, therefore, further thinning of the overlying tree canopy and, consequently, more insolation at the ground surface. These processes and feedback mechanisms are critical in the generation of collapse scars in stage III.

Differing ground surface properties, particularly albedo, can amplify the differences in incoming shortwave radiation among the land covers. However, the difference in mean albedo during the snow-free season (May–September) below the plateau canopies is less than 5 % and displays a small increasing gradient as the canopy becomes more dense (sparse – 0.111; intermediate – 0.127; dense: 0.147). The mean wetland albedo (0.145) during the snow-free season is also similar to the plateau surfaces and most closely resembles the surface albedo of the dense plateau. The greatest contrast in albedo occurs during the period of several weeks while snow still covers the plateaus but is absent on the adjacent wetlands (Connon et al., 2021). This contrast in albedo is also evident in Fig. 7b, which shows that, following winter, outgoing shortwave radiation from the wetland increases before the forested stations. Helbig et al. (2016b) attributed their observed increase in landscape albedo in this late winter/spring period to the permafrost-thaw-induced conversion of forest (lower albedo) to wetland (higher albedo) and suggested that this could lead to a regional cooling effect during this time of the year. However, that study implicitly assumed that the wetlands were a final land cover stage rather than an incremental step toward the reestablishment of forest as depicted in the conceptual framework presented in Fig. 6.

4.2.3 Hydrological characteristics

As the land covers presented in the conceptual framework transition from one to the next, hydrological processes also change (Fig. 6a). In the early stages (I and II), a relatively large proportion of hydrological inputs from the atmosphere are stored in collapse scars due to their impoundment by the permafrost on their margins (Connon et al., 2014). Evapotranspiration from the landscape is relatively low, given the high proportion of forest and relatively low transpiration by the black spruce that dominates the plateau canopies (Warren et al., 2018). In the early land cover stages (I and II) when forests predominate, understorey vegetation provide the pathway for evapotranspiration (Chasmer et al., 2011). The incremental change in land covers presented in Fig. 6 involves biophysical changes that affect the partitioning of precipitation into storage or runoff. By stage III to IV, wetlands are interconnected and rapidly expanding, and the storage of water on the landscape reaches its minimum level, while runoff from the landscape is maximized (Fig. 6a). This increased runoff is enabled by the removal of permafrost barriers (Haynes et al., 2018) and areal expansion of runoff contributing areas resulting in greater hydrological connectivity and, therefore, drainage of the landscape (Connon et al., 2014). These observations coincide with a period of steady, unchanging annual precipitation; therefore, precipitation does not account for elevated basin runoff (Connon et al., 2014). A decrease in landscape drainage then follows in the subsequent stages as the transient runoff contributions from captured collapse scars diminish as the importance of evapotranspiration increases as the wetlands become the predominant land cover (IV and V). The increase in evapotranspiration is due to increases in evaporation from areas occupied by standing water and saturated or near-saturated wetland vegetation, including *Sphagnum* mosses, with losses due to transpiration driven by shrub vegetation (Warren et al., 2018). In the advanced stages (VI and VII) evapotranspiration would decrease as a result of the drier wetland surfaces as hummock microtopography replaces saturated *Sphagnum* lawns. The treed (afforested) wetlands (VII) have not been studied to the same degree as peat plateaus or collapse scar wetlands (Haynes et al., 2020; Disher et al., 2021), and therefore, ground-based hydrological data specific to these features are lacking.

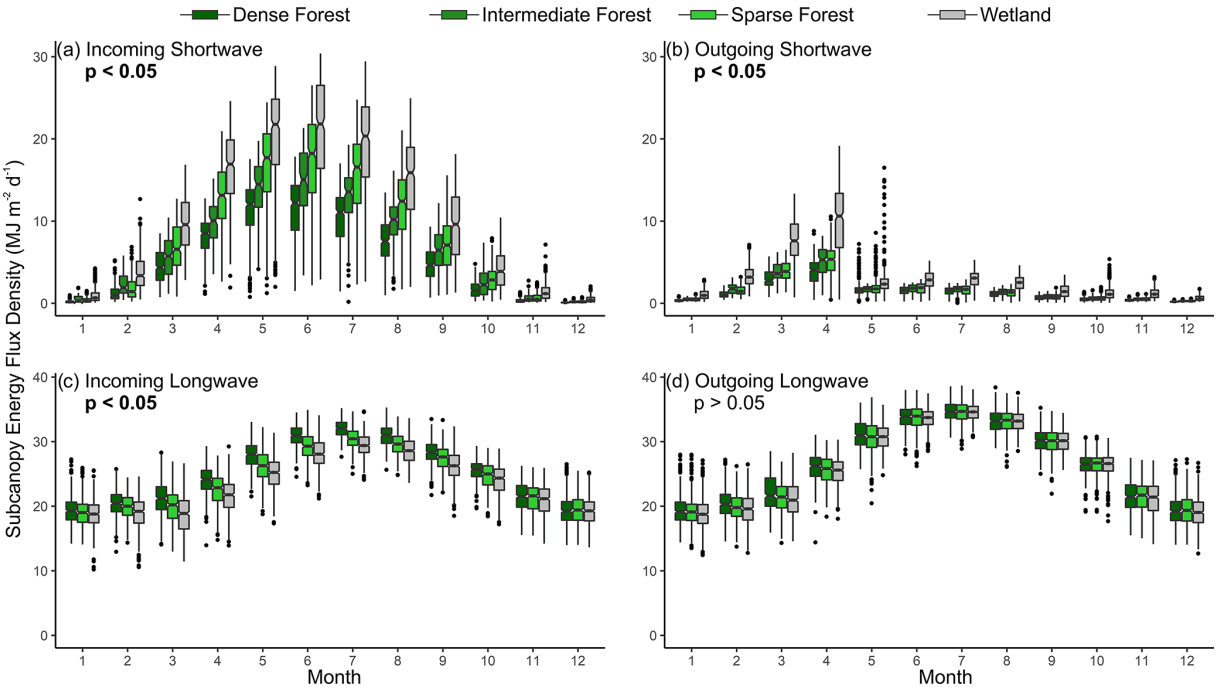

Figure 7. Subcanopy daily total (megajoules per square metre per day) incoming shortwave **(a)**, outgoing shortwave **(b)**, incoming longwave **(c)**, and outgoing longwave **(d)** at the four meteorological stations. Each station represents a distinct land cover, i.e. dense forest (2007–2019), intermediate forest (2014–2019), sparse forest (2015–2018), and treeless wetland (2004–2019). The boxes represent the 25th and 75th percentile, while the whiskers represent the range of the data. The notches on each box indicate the confidence interval ($a = 0.05$) around the mean, while the statistical differences between meteorological stations have been presented in the upper left of each plot as determined by one-way ANOVA. Significant p values have been highlighted with bold text.

5 Conclusions

The discontinuous permafrost zone of the Taiga Plains exemplifies a landscape in transition. Coupling a broad-scale mapping initiative with the detail of site-specific data collected in the Scotty Creek basin demonstrates a permafrost-thaw-induced land cover transition. This transition is incremental and involves distinct land cover stages. The first and last of these is a continuous forest cover, although in the first stage the forest is underlain by permafrost, while in the last stage it is not. Unlike traditional concepts of land cover change in peatland-dominated regions of discontinuous permafrost in which forest reestablishment occurs over centuries and is constrained by the rate of permafrost redevelopment, the concept presented here described forest reestablishment within decades and resulting from continued permafrost thaw, a process which allows wetlands to dewater sufficiently for tree growth. Each land cover stage has characteristic biophysical, hydrological, and micrometeorological features.

The proposed conceptual framework of landscape evolution describes the transitions occurring across the Taiga Plains in peat plateau–collapse scar wetland complexes like Scotty Creek. This study also identifies the applicability of this conceptual framework across a large region of the Canadian north. We establish the likely pattern of change across these peat plateau–collapse scar wetland complexes and project their future trajectory by combining long-term field observations with analyses of contemporary and historical imagery. It is proposed that, while permafrost-thaw-induced land cover changes have previously been dominated by a transition from forest to wetland, this transition is not permanent, and forested land covers are likely to return over time, although they are unlikely to be underlain by permafrost. This research improves the understanding of how peat plateau–collapse scar wetland complexes in the Taiga Plains may be impacted by ongoing permafrost thaw, and these results may also be of relevance to other peatland-rich permafrost environments across the circumpolar north.

Data availability. The radiation flux data used in this paper are catalogued for open access in the Wilfrid Laurier University (WLU) Data Repository at https://doi.org/10.5683/SP2/JTIQDO (Carpino and Quinton, 2021).

Author contributions. All authors contributed to the development of the research question and the methodological approach used in this study. OC and RC performed the analyses. OC, KH, and WQ wrote the paper, with input and editorial contributions from RC, JC, and ÉD.

Competing interests. The authors declare that they have no conflict of interest.

Disclaimer. Publisher's note: Copernicus Publications remains neutral with regard to jurisdictional claims in published maps and institutional affiliations.

Acknowledgements. We gratefully acknowledge the support of the Dehcho First Nations, particularly the Liidlii Kue First Nation and Jean Marie River First Nation. We also thank these communities for their long-standing support of the Scotty Creek Research Station. This work was funded by ArcticNet through their support of the Dehcho Collaborative on Permafrost (DCoP), and by the Natural Sciences and Engineering Research Council of Canada (NSERC). We also acknowledge the Canada Foundation for Innovation (CFI) for providing funding for infrastructure critical to this study.

Financial support. This research has been supported by the ArcticNet (Project02 (2018) grant) and the Natural Sciences and Engineering Research Council of Canada (grant no. RGPIN-2020-07229).

Review statement. This paper was edited by Laurent Pfister and reviewed by two anonymous referees.

References

Baltzer, J., Veness, T., Chasmer, L., Sniderhan, A., and Quinton, W.: Forests on thawing permafrost: Fragmentation, edge effects, and net forest loss, Global Change Biol., 20, 824–834, https://doi.org/10.1111/gcb.12349, 2014.

Beilman, D., Vitt, D., and Halsey, L.: Localized Permafrost Peatlands in Western Canada: Definition, Distributions, and Degradation, Arct. Antarct. Alp. Res., 33, 70–77, https://doi.org/10.1080/15230430.2001.12003406, 2001.

Beilman, D. W. and Robinson, S. D.: Peatland permafrost thaw and landcover type along a climate gradient, in: Proceedings of the Eighth International Conference on Permafrost, edited by: Phillips, M., Springman, S. M., and Arenson, L. U., Balkema, Zurich, Switzerland, 61–65, 21–25 July 2003.

Biskaborn, B. K., Smith, S. L., Noetzli, J., Matthes, H., Vieira, G., Streletskiy, D. A., Schoeneich, P., Romanovsky, V. E., Lewkowicz, A. G., Abramov, A., Allard, M., Boike, J., Cable, W. L., Christiansen, H. H., Delaloye, R., Diekmann, B., Drozdov, D., Etzelmüller, B., Grosse, G., Guglielmin, M., Ingeman-Nielsen, T., Isaksen, K., Ishikawa, M., Johansson, M., Johannsson, H., Joo, A., Kaverin, D., Kholodov, A., Konstantinov, P., Kröger, T., Lambiel, C., Lanckman, J. P., Luo, D., Malkova, G., Meiklejohn, I., Moskalenko, N., Oliva, M., Phillips, M., Ramos, M., Sannel, A. B. K., Sergeev, D., Seybold, C., Skryabin, P., Vasiliev, A., Wu, Q., Yoshikawa, K., Zheleznyak, M., and Lantuit, H.: Permafrost is warming at a global scale, Nat. Commun., 10, 264, https://doi.org/10.1038/s41467-018-08240-4, 2019.

Bolin Centre for Climate Research: The Northern Circumpolar Soil Carbon Database, available at: https://bolin.su.se/data/ncscd/ (last access: 20 March 2019), 2013.

Box, J. E., Colgan, W. T., Christensen, T. R., Schmidt, N. M., Lund, M., Parmentier, F. W., Brown, R., Bhatt, U. S., Euskirchen, E. S., Romanovsky, V. E., Walsh, J. E., Overland, J. E., Wang, M., Corell, R. W., Meier, W. N., Wouters, B., Mernild, S., Mård, J., Pawlak, J., and Olsen, M. S.: Key indicators of arctic climate change: 1971–2017, Environ. Res. Lett., 14, 045010, https://doi.org/10.1088/1748-9326/aafc1b, 2019.

Brown, R. J. E.: Permafrost Investigations on the Mackenzie Highway in Alberta and Mackenzie District, Technical Paper No. 175, Division of Building Research, National Research Council, 1–71, Ottawa, Canada, 1964.

Brown, J., Ferrians, O., Heginbottom, J. A., and Melnikov, E.: Circum-Arctic Map of Permafrost and Ground-Ice Conditions, Version 2 [Permaice subset used], National Snow and Ice Data Center (NSIDC), Boulder, Colorado, USA, 2002.

Camill, P.: Peat accumulation and succession following permafrost thaw in the boreal peatlands of Manitoba, Canada, Ecoscience, 6, 592–602, 1999.

Camill, P.: How much do local factors matter for predicting transient ecosystem dynamics? Suggestions from permafrost formation in boreal peatlands, Global Change Biol., 6, 169–182, https://doi.org/10.1046/j.1365-2486.2000.00293.x, 2000.

Camill, P. and Clark, J. S.: Climate change disequilibrium of boreal permafrost peatlands caused by local processes, Am. Nat., 151, 207–222, https://doi.org/10.1086/286112, 1998.

Carpino, O. A., Berg, A. A., Quinton, W. L., and Adams, J. R.: Climate change and permafrost thaw- induced boreal forest loss in northwestern Canada, Environ. Res. Lett., 13, 084018, https://doi.org/10.1088/1748-9326/aad74e, 2018.

Carpino, O. and Quinton, W.: Four Component Radiation Data at Scotty Creek, NWT, Canada 2004–2019, https://doi.org/10.5683/SP2/JTIQDO, 2021.

Chasmer, L. and Hopkinson, C.: Threshold loss of discontinuous permafrost and landscape evolution, Global Change Biol., 23, 2672–2686, 2017.

Chasmer, L., Hopkinson, C., and Quinton, W.: Quantifying errors in discontinuous permafrost plateau change from optical data, Northwest Territories, Canada: 1947–2008, Can. J. Remote Sens., 36, 211–223, https://doi.org/10.1111/gcb.13537, 2010.

Chasmer, L., Quinton, W., Hopkinson, C., Petrone, R., and Whittington, P.: Vegetation Canopy and Radiation Controls on Permafrost Plateau Evolution within the Discontinuous Permafrost Zone, Northwest Territories, Canada, Permafrost Periglac., 22, 199–213, https://doi.org/10.1002/ppp.724, 2011.

Connon, R. F., Quinton, W. L., Craig, J. R., and Hayashi, M.: Changing hydrologic connectivity due to permafrost thaw in the lower Liard River valley, NWT, Canada, Hydrol. Process., 28, 4163–4178, https://doi.org/10.1002/hyp.10206, 2014.

Connon, R. F., Quinton, W. L., Craig, J. R., Hanisch, J., and Sonnentag, O.: The hydrology of interconnected bog complexes in discontinuous permafrost terrains, Hydrol. Process., 29, 3831–3847, https://doi.org/10.1002/hyp.10604, 2015.

Connon, R. F., Devoie, É., Hayashi, M., Veness, T., and Quinton, W.: The influence of shallow taliks on permafrost thaw and active layer dynamics in subarctic Canada, J. Geophys. Res.-Earth, 123, 281–297, https://doi.org/10.1002/2017JF004469, 2018.

Connon, R. F., Chasmer, L. E., Haughton, E., Helbig, M., Hopkinson, C., Sonnentag, O., and Quinton, W. L.: The implications of permafrost thaw and land cover change on snow water equivalent accumulation, melt and runoff in discontinuous permafrost peatlands, Hydrol. Process., submitted, 2021.

Devoie, É. G., Craig, J. R., Connon, R. F., and Quinton, W. L.: Taliks: A tipping point in discontinuous permafrost degradation in peatlands, Water Resour. Res., 55, 9838–9857, https://doi.org/10.1029/2018WR024488, 2019.

Disher, B. S.: Characterising the hydrological function of treed bogs in the zone of discontinuous permafrost, M.Sc. Thesis, Wilfrid Laurier University, Waterloo, Ontario, Canada, 72 pp., 2020.

Disher, B. S., Connon, R. F., Haynes, K. M., Hopkinson, C., and Quinton, W. L.: The hydrology of treed wetlands in thawing discontinuous permafrost regions, Ecohydrology, e2296, https://doi.org/10.1002/eco.2296, 2021.

Dymond, S. F., D'Amato, A. W., Kolka, R. K., Bolstad, P. V., Sebestyen, S. D., Gill, K., and Curzon, M. T.: Climatic controls on peatland black spruce growth in relation to water table variation and precipitation, Ecohydrology, 12, e2137, https://doi.org/10.1002/eco.2137, 2019.

Environment and Climate Change Canada: Adjusted and homogenized Canadian climate data, available at: https://www.canada.ca/en/environment-climate-change/services/climate-change/science-research-data/climate-trends-variability/adjusted-homogenized-canadian-data.html, last access: 1 June 2020.

Eppinga, M. B., Rietkerk, M., Wassen, M. J., and De Ruiter, P. C.: Linking habitat modification to catastrophic shifts and vegetation patterns in bogs, Plant Ecol., 200, 53–68, https://doi.org/10.1007/s11258-007-9309-6, 2007.

Garon-Labreque, M. É., Léveillé-Bourret, É., Higgins, K., and Sonnentag, O.: Additions to the boreal flora of the Northwest Territories with a preliminary vascular flora of Scotty Creek, Can. Field Nat., 129, 349–367, https://doi.org/10.22621/cfn.v129i4.1757, 2015.

Gibson, C. M., Chasmer, L. E., Thompson, D. K., Quinton, W. L., Flannigan, M. D., and Olefeldt, D.: Wildfire as a major driver of recent permafrost thaw in boreal peatlands, Nat. Commun., 9, 3041, https://doi.org/10.1038/s41467-018-05457-1, 2018.

Halsey, L. A., Vitt, D. H., and Zoltai, S. C.: Disequilibrium response of permafrost in boreal continental western Canada to climate change, Climatic Change, 30, 57–73, https://doi.org/10.1007/BF01093225, 1995.

Hayashi, M., Quinton, W. L., Pietroniro, A., and Gibson, J. J.: Hydrologic functions of wetlands in a discontinuous permafrost basin indicated by isotopic and chemical signatures, J. Hydrol., 296, 81–97, https://doi.org/10.1016/j.jhydrol.2004.03.020, 2004.

Hayashi, M., Goeller, N., Quinton, W. L., and Wright, N.: A simple heat-conduction method for simulating the frost-table depth in hydrological models, Hydrol. Process., 21, 2610–2622, https://doi.org/10.1002/hyp.6792, 2007.

Haynes, K. M., Connon, R. F., and Quinton, W. L.: Permafrost thaw induced drying of wetlands at Scotty Creek, NWT, Canada, Environ. Res. Lett., 13, 114001, https://doi.org/10.1088/1748-9326/aae46c, 2018.

Haynes, K. M., Connon, R. F., and Quinton, W. L.: Hydrometeorological measurements in peatland-dominated, discontinuous permafrost at Scotty Creek, Northwest Territories, Canada, Geosci. Data J., 6, 85–96, https://doi.org/10.1002/gdj3.69, 2019.

Haynes, K. M., Smart, J., Disher, B., Carpino, O., and Quinton, W. L.: The role of hummocks in re- establishing black spruce forest following permafrost thaw, Ecohydrology, 14, e2273, https://doi.org/10.1002/eco.2273, 2020.

Helbig, M., Pappas, C., and Sonnentag, O.: Permafrost thaw and wildfire: Equally important drivers of boreal tree cover changes in the Taiga Plains, Canada, Geophys. Res. Lett., 43, 1598–1606, https://doi.org/10.1002/2015GL067193, 2016a.

Helbig, M., Wischnewski, K., Kljun, N., Chasmer, L. E., Quinton, W. L., Detto, M., and Sonnentag, O.: Regional atmospheric cooling and wetting effect of permafrost thaw- induced boreal forest loss, Global Change Biol., 22, 4048–4066, https://doi.org/10.1111/gcb.13348, 2016b.

Holloway, J. E. and Lewkowicz, A. G.: Half a century of discontinuous permafrost persistence and degradation in western Canada, Permafrost Periglac., 31, 85–96, https://doi.org/10.1002/ppp.2017, 2019.

Hugelius, G., Bockheim, J. G., Camill, P., Elberling, B., Grosse, G., Harden, J. W., Johnson, K., Jorgenson, T., Koven, C. D., Kuhry, P., Michaelson, G., Mishra, U., Palmtag, J., Ping, C.-L., O'Donnell, J., Schirrmeister, L., Schuur, E. A. G., Sheng, Y., Smith, L. C., Strauss, J., and Yu, Z.: A new data set for estimating organic carbon storage to 3 m depth in soils of the northern circumpolar permafrost region, Earth Syst. Sci. Data, 5, 393–402, https://doi.org/10.5194/essd-5-393-2013, 2013a.

Hugelius, G., Tarnocai, C., Broll, G., Canadell, J. G., Kuhry, P., and Swanson, D. K.: The Northern Circumpolar Soil Carbon Database: spatially distributed datasets of soil coverage and soil carbon storage in the northern permafrost regions, Earth Syst. Sci. Data, 5, 3–13, https://doi.org/10.5194/essd-5-3-2013, 2013b.

Iversen, C. M., Childs, J., Norby, R. J., Ontl, T. A., Kolka, R. K., Brice, D. J., McFarlane, K. J., and Hanson, P. J.: Fine-root growth in a forested bog is seasonally dynamic, but shallowly distributed in nutrient-poor peat, Plant Soil, 424, 123–143, https://doi.org/10.1007/s11104-017-3231-z, 2018.

Ketteridge, N., Thompson, D. K., Bombonato, L., Turetsky, M. R., Benscoter, B. W., and Waddington, J. M.: The ecohydrology of forested peatlands: simulating the effects of tree shading on moss evaporation and species composition, J. Geophys. Res.-Biogeo., 118, 422–435, https://doi.org/10.1002/jgrg.20043, 2013.

Kokelj, S. V., Palmer, M. J., Lantz, T. C., and Burn, C. R.: Ground Temperatures and Permafrost Warming from Forest to Tundra, Tuktoyaktuk Coastlands and Anderson Plain, NWT, Canada, Permafrost Periglac., 28, 543–551, https://doi.org/10.1002/ppp.1934, 2017.

Korosi, J. B., Thienpont, J. R., Pisaric, M. F. J., deMontigny, P., Perreault, J. T., McDonald, J., Simpson, M. J., Armstrong, T., Kokelj, S. V., Smol, J. P., and Blais, J. M.: Broad-scale lake expansion and flooding inundates essential wood bison habitat, Nat. Commun., 8, 14510, https://doi.org/10.1038/ncomms14510, 2017.

Kurylyk, B., Hayashi, M., Quinton, W., McKenzie, J., and Voss, C.: Influence of vertical and lateral heat transfer on permafrost thaw, peatland landscape transition, and groundwater flow, Water Resour. Res., 52, 1286–1305, https://doi.org/10.1002/2015WR018057, 2016.

Kwong, J. T. and Gan, T. Y.: Northward migration of permafrost along the Mackenzie Highway and climatic warming, Climate Change, 26, 399–419, https://doi.org/10.1007/BF01094404, 1994.

Lieffers, V. J. and Rothwell, R. L.: Rooting of peatland black spruce and tamarack in relation to depth of water table, Can. J. Botany, 65, 817–821, 1987.

Loisel, J. and Yu, Z.: Surface vegetation patterning controls carbon accumulation in peatlands, Geophys. Res. Lett., 40, 5508–5513, https://doi.org/10.1002/grl.50744, 2013.

McClymont, A. F., Hayashi, M., Bentley, L. R., and Christensen, B. S.: Geophysical imaging and thermal modeling of subsurface morphology and thaw evolution of discontinuous permafrost, J. Geophys. Res.-Earth, 118, 1826–1837, https://doi.org/10.1002/jgrf.20114, 2013.

McKenzie, J. M. and Voss, C. I.: Permafrost thaw in a nested groundwater-flow system, Hydrogeol. J., 21, 299–316, 2013.

Mekis, É. and Vincent, L. A.: An overview of the second generation adjusted daily precipitation dataset for trend analysis in Canada, Atmos. Ocean, 49, 163–177, https://doi.org/10.1080/07055900.2011.583910, 2011.

Natural Resources Canada: Wooded areas, saturated soils and landscape in Canada – CanVec series – Land features, available at: https://open.canada.ca/data/en/dataset/80aa8ec6-4947-48de-bc9c-7d09d48b4cad (last access: 10 July 2019), 2017.

NWWG.: Wetlands of Canada, Ecological Land Classification Series No. 24, Sustainable Development Branch, Environment Canada, Polyscience Publications Inc., Québec, Canada, 452 pp., 1988.

Olefeldt, D., Persson, A., and Turetsky, M. R.: Influence of the permafrost boundary on dissolved organic matter characteristics in rivers within the Boreal and Taiga plains of western Canada, Environ. Res. Lett., 9, 035005, https://doi.org/10.1088/1748-9326/9/3/035005, 2014.

Olefeldt, D., Goswami, S., Grosse, G., Hayes, D., Hugelius, G., Kuhry, P., McGuire, A. D., Romanovsky, V. E., Sannel, A. B. K., Schuur, E. A. G., and Turetsky, M. R.: Circumpolar distribution and carbon storage of thermokarst landscapes, Nat. Commun., 7, 13043, https://doi.org/10.1038/ncomms13043, 2016.

Overland, J. E., Hanna, E., Hanssen-Bauer, I., Kim, S. J., Walsh, J. E., Wang, M., Bhatt, U. S., Thoman, R. L., and Ballinger, T. J.: Surface Air Temperature, in: Arctic Report Card 2019, edited by: Richter-Menge, J., Druckenmiller, M. L., and Jeffries, M., available at: https://arctic.noaa.gov/Report-Card/Report-Card-2019 (last access: 11 July 2020), 2019.

Pelletier, N., Talbot, J., Olefeldt, D., Turetsky, M., Blodau, C., Sonnentag, O., and Quinton, W. L.: Influence of Holocene permafrost aggradation and thaw on the paleoecology and carbon storage of a peatland complex in northwestern Canada, Holocene, 27, 1391–1405, https://doi.org/10.1177/0959683617693899, 2017.

Porter, T. J., Schoenemann, S. W., Davies, L. J., Steig, E. J., Bandara, S., and Froese, D. G.: Recent summer warming in northwestern Canada exceeds the Holocene thermal maximum, Nat. Commun., 10, 1631, https://doi.org/10.1038/s41467-019-09622-y, 2019.

Quinton, W., Berg, A., Braverman, M., Carpino, O., Chasmer, L., Connon, R., Craig, J., Devoie, É., Hayashi, M., Haynes, K., Olefeldt, D., Pietroniro, A., Rezanezhad, F., Schincariol, R., and Sonnentag, O.: A synthesis of three decades of hydrological research at Scotty Creek, NWT, Canada, Hydrol. Earth Syst. Sci., 23, 2015–2039, https://doi.org/10.5194/hess-23-2015-2019, 2019.

Quinton, W. L., Hayashi, M., and Chasmer, L. E.: Peatland hydrology of discontinuous permafrost in the Northwest Territories: overview and synthesis, Can. Water Resour. J., 34, 311–328, https://doi.org/10.4296/cwrj3404311, 2009.

Quinton, W. L., Hayashi, M., and Chasmer, L.: Permafrost-thaw-induced land- cover change in the Canadian subarctic: Implications for water resources, Hydrol. Process., 25, 152–158, https://doi.org/10.1002/hyp.7894, 2011.

Robinson, S. D. and Moore, T. R.: The influence of permafrost and fire upon carbon accumulation in high boreal peatlands, Northwest Territories, Canada, Arct. Antarct. Alp. Res., 32, 155–166, https://doi.org/10.1080/15230430.2000.12003351, 2000.

Rowland, J. C., Jones, C. E., Altmann, G., Bryan, R., Crosby, B. T., Hinzman, L. D., Kane, D. L., Lawrence, D. M., Mancino, A., Marsh, P., McNamara, J. P., Romanvosky, V. E., Toniolo, H., Travis, B. J., Trochim, E., Wilson, C. J., and Geernaert, G. L.: Arctic Landscapes in Transition: Responses to Thawing Permafrost, 91, 229–230, https://doi.org/10.1029/2010EO260001, 2010.

St. Jacques, J. M. and Sauchyn, D. J.: Increasing winter baseflow and mean annual streamflow from possible permafrost thawing in the Northwest Territories, Canada, Geophys. Res. Lett., 36, L01401, https://doi.org/10.1029/2008GL035822, 2009.

Stofferahn, E., Fisher, J. B., Haynes, D. J., Schwalm, C. R., Huntzinger, D. N., Hantson, W., Poulter, B., and Zhang, Z.: The Arctic-Boreal vulnerability experiment model benchmarking system, Environ. Res. Lett., 14, 055002, https://doi.org/10.1088/1748-9326/ab10fa, 2019.

Thie, J.: Distribution and thawing of permafrost in the southern part of the discontinuous permafrost zone in Manitoba, Arctic Journal of the Arctic Institute of North America, 34, 189–200, https://doi.org/10.14430/arctic2873, 1974.

Treat, C. C. and Jones, M. C.: Near-surface permafrost aggradation in Northern Hemisphere peatlands shows regional and global trends during the past 6000 years, Holocene, 28, 998–1010, https://doi.org/10.1177/0959683617752858, 2018.

Vincent, L. A., Wang, X. L., Milewska, E. J., Wan, H., Yang, F., and Swail, V.: A second generation of homogenized Canadian monthly surface air temperature for climate trend analysis, J. Geophys. Res.-Atmos., 117, D18110, https://doi.org/10.1029/2012JD017859, 2012.

Vincent, L. A., Zhang, X., Brown, R., Feng, Y., Mekis, E., Milewska, E., Wan, H., and Wang, X.: Observed trends in Canada's climate and influence of low-frequency variability modes, J. Climate, 28, 4545–4560, https://doi.org/10.1175/JCLI-D-14-00697.1, 2015.

Vitt, D. H., Halsey, L. A., and Zoltai, S. C.: The bog landcovers of continental Western Canada in relation to climate and permafrost patterns, Arct. Antarct. Alp. Res., 26, 1–13, https://doi.org/10.1080/00040851.1994.12003032, 1994.

Vonk, J. E., Tank, S. E., and Walvoord, M. A.: Integrating hydrology and biogeochemistry across frozen landscapes, Nat. Commun., 10, 5377, https://doi.org/10.1038/s41467-019-13361-5, 2019.

Walvoord, M. A. and Kurylyk, B.: Hydrologic Impacts of Thawing Permafrost – A Review, Vadose Zone J., 15, 1–20, https://doi.org/10.2136/vzj2016.01.0010, 2016.

Warren, R. K., Pappas, C., Helbig, M., Chasmer, L. E., Berg, A. A., Baltzer, J. L., Quinton, W. L., and Sonnetag, O.: Minor contribution of overstory transpiration to landscape evapotranspiration in boreal permafrost peatlands, Ecohydrology, 11, 1975, https://doi.org/10.1002/eco.1975, 2018.

Webster, C., Rutter, N., Zahnner, F., and Jonas, T.: Measurement of Incoming Radiation below Forest Canopies: A Comparison of Different Radiometer Configurations, J. Hydrometeorol., 17, 853–864, https://doi.org/10.1175/JHM-D-15-0125.1, 2016.

Wright, N., Hayashi, M., and Quinton, W.: Spatial and temporal variations in active layer thawing and their implication on runoff generation in peat-covered permafrost terrain, Water Resour. Res., 45, W05414, https://doi.org/10.1029/2008WR006880, 2009.

Zoltai, S. C.: Cyclic development of permafrost in the peatlands of Northwestern Alberta, Canada, Arct. Antarct. Alp. Res., 25, 240–246, https://doi.org/10.1080/00040851.1993.12003011, 1993.

Zoltai, S. C. and Tarnocai, C.: Perennially frozen peatlands in the Western Arctic and Subarctic of Canada, Can. J. Earth Sci., 12, 28–43, https://doi.org/10.1139/e75-004, 1975.